

Hysteretic Behaviour Simulation of Low-Yield Steels Under Mechanical Cyclic Loads

Eber Pérez Isidro¹, Israel Aarón Palma Quiroz²,
Jesús Emmanuel Cerón Carballo³.
Academic Area of Engineering and Architecture
Autonomous University of Hidalgo
Mineral de la Reforma, Hidalgo, Mexico^{1,2,3}

Jorge Humberto Chávez Gómez⁴.
Faculty of Civil Engineering
Autonomous University of Nuevo Leon
Nuevo Leon, Mexico⁴

Abstract— The purpose of this work is to analyse the behaviour of steels of Low Yield Point (LYP), applying mechanical cyclic loads. To define the cyclic behaviour and obtain the behaviour of resistance, ductility and energy dissipation, numerical simulations were carried out of two structural steels (LYP100 and LYP160) and a conventional steel (Q235B), applying monotonic and cyclic loading patterns, using the analytical model by nonlinear kinematic hardening for Mróz-Garud stress fields. The results obtained in this study show consistency with recent publications, revealing that, despite the low elastic limit of the LYP steels, they improve their cyclic, ductile and energy dissipation responses, important for the control of the seismic response.

Keywords—Low yield point steel; hardening cinematic; cyclic behavior.

I. INTRODUCTION

The analysis of the behaviour of advanced structural materials plays an important role in the structural design for energy dissipation. The structural elements destined to the dissipation of energy are known as control systems. Among these control systems are the passive control systems, which are economical and effective in reducing structural deformation during earthquakes [1]. The control of the dissipation of energy in buildings, consists of adding dissipaters that allow to distribute the demand of ductility in a rational way, forming special points that dissipate energy in stable form and that can be repaired [2].

In the literature there are a significant number of energy dissipaters manufactured with conventional steel plates and copper, among the most important we can find the devices Added Damping and Stiffness (ADAS) [3], the Triangular Added Damping And Stiffness (TADAS) [4], the Slit Damper [5] and the copper-based Bi-directional Energy Dissipation Device (Cu-BEDD) [2]. On the other hand, as the ideal material for the dissipation of energy, steels with low yield point (LYP) have been developed, and these steels are studied for the field of seismic engineering. In [6] the authors studied several configurations of shear walls made of steel LYP100, focusing on the capacity of energy dissipation, ductility, out-of-plane deformation and the effect of the stress field on columns. Throughout experimental tests with quasi-static loads and a numerical method, the results show the performance of the walls exposing improvement in the dissipation capacity, energy and ductility, in addition, one of their configuration (shear wall with T-type stiffeners), shows the greatest decrease in the impact of stresses on the columns. In [7] the authors propose an innovative beam for the coupling of shear walls and formulate a trilinear hysteretic model, which simulates the cyclic behaviour; the

analytical and experimental results show an excellent performance by hysteresis, increasing the energy dissipation up to 94% and a rigidity reduction of 27.3%, compared with coupling beams manufactured in conventional steel. A probabilistic study was developed by [8], this study addresses the seismic performance, hysteresis and vulnerability applied to shear walls, manufactured in steel LYP100. Through fragility analysis, the authors obtained an improvement in seismic performance and a reduction in seismic vulnerability. On the other hand, the same authors in [9]–[11] studied the behaviour by buckling, creep, hysteresis and aspect ratio of LYP steel plates, under various support and load conditions, the experimental and numerical results provided practical recommendations for the seismic design.

Likewise, when a structure is subjected to seismic conditions, the energy dissipation elements undergo plastic deformations, where, their magnitude will depend mainly on the number of repeated cycles during the event, which will eventually lead to fatigue of the material [12], [13]. The potential of the LYP steels has motivated several studies to dissipate energy, e.g., in [14] the authors study experimentally and with the Finite Element Method (FEM), fatigue behaviour and hysteresis in the Nonstiffener Shear Panel Dampers manufactured in steel LYP100, the authors report a good performance due to fatigue in monotonic and increasing load cycles. Metal shock absorbers made of steel LYP100, LYP160 and LYP225 are studied in [15], the results show a behaviour of plasticity and energy dissipation by hysteresis. A variant of the ADAS device is studied in [16] called Two-stage Energy Dissipation Device, manufactured with two types of steel plates (Q235 on its periphery and LYP steel plates as core); the authors report geometric parameters that affect the dissipation of energy by hysteresis, in addition to a force-restorative model applicable to this type of dissipater. In [17], the authors propose a connection system called Posttensioned Energy Dissipation (PTED) with bolted angles in the upper part and one in the lower part made of LYP100 steel. This system works as an energy dissipater, minimizing post-earthquake damage and residual deformations. The analyzes are carried out under various modes of failure and cyclical loads. The local buckling of the beam, the deformations in the strands and the fracture angle are taken into account for the analysis. The analytical and experimental results showed that the failure modes can be captured with sufficient precision, showing a significant improvement by postponing the fracture point from 4% to 7%, in addition, the energy dissipation capacity was increased by 222% in Comparison with A572 steels.

TABLE I. MECHANICAL PROPERTIES OF LYP STEEL, [23], [24]

Material (steel)	Specimen number	Elasticity module, E , (N/mm ²)	Yield point, f_y , (N/mm ²)	Ultimate resistance, f_u , (N/mm ²)	Cyclic force coefficient, K' , (N/mm ²)	Exponent cyclical force, n'
LYP100	A-1	191,600.0	75	241	155.57	0.39
	A-2	201,300.0	75	256	137.96	0.40
	A-9	194,500.0	81	241	160.77	0.45
LYP160	B-1	195,700.0	99	272	205.56	0.20
	B-2	211,100.0	97	252	160.02	0.45
	B-9	204,533.0	114	291	181.40	0.35
Q235	C-1	189,605.87	231.66	514	1,096.26	0.249
	C-2	189,605.87	231.66	514	1,096.26	0.249
	C-3	189,605.87	231.66	514	1,096.26	0.249

TABLE I. CHEMIST COMPOSITION OF LYP STEEL, [23]

Material (steel)	Chemist composition (%)							
	C 10^{-2}	Si 10^{-2}	Mn 10^{-2}	P 10^{-3}	S 10^{-3}	Als 10^{-3}	Ti 10^{-2}	Pcm 10^{-2}
LYP100	0.12	1.0	5.0	10.0	4.0	37.0	4.2	13.0
LYP160	0.28	4.0	18.0	11.0	4.0	25.0	3.4	0.11
Q235B	0.16	0.26	0.45	0.021	0.025	-	-	-

1

In addition, mechanical studies and constitutive models such as that of Chaboche [18] and Hu [19], [20]) for steel plates LYP100, LYP160 and LYP225, were studied in [21]. In this work, the steels were tested under 12 load patterns to observe their monotonic response, deformation capacity and energy dissipation by hysteresis. The experimental and numerical results indicated a high performance, providing reliable constitutive models for simulation in engineering applications. In [22] these steels were also experimentally studied, under different amplitudes of constant deformation, the results provided parameters for the relationship of Coffin-Manson and the Koruda model, obtaining data for the analysis by cyclic hardening and cyclical stress-strain response.

All these studies and results show that the ductility and the capacity of energy dissipation of the LYP steels are of consideration, where, the hardening by cyclic deformation plays a fundamental role in its response, that is, the cyclic response differs with respect to the increasing monotonic response, indicating that cyclical behavior can not be inferred from

monotonic behavior. Therefore, it is essential to study the cyclic behavior of LYP steels so they can be modeled accurately and used in structural design. In particular, in the time-history analysis, where precise models are required to study and simulate the material in the global structural response.

This work began with the study of the behavior of the LYP steels under repeated amplitudes of effort, limited to that the failure was generated by bending, without taking into account the failure by shear and torsion. Using experimental data obtained in [23] and [24], numerical simulations of the specimens LYP100, LYP160 and Q235B were performed, the latter equivalent to conventional A36 steel. The steels were subjected to three load patterns, seeking to study the cyclic characteristics, focusing on the response capacity of hardening, ductility and dissipation of cyclic energy. The Ramberg-Osgood model was used to obtain the theoretical stress-strain curves of the material obtaining hardening parameters. The results obtained from the Ramberg-Osgood model were applied in the non-linear kinematic hardening model of Mróz-Garud, considering the isotropic and kinematic components, to simulate the hysteresis behavior in the LYP and Q235B steels under cyclic loads. The results obtained were compared with those reported in [23] and [24], indicating a good consistency in the experimental and analytical results. In addition, the comparison of the behavior of the LYP steels with the conventional steel Q235B is made.

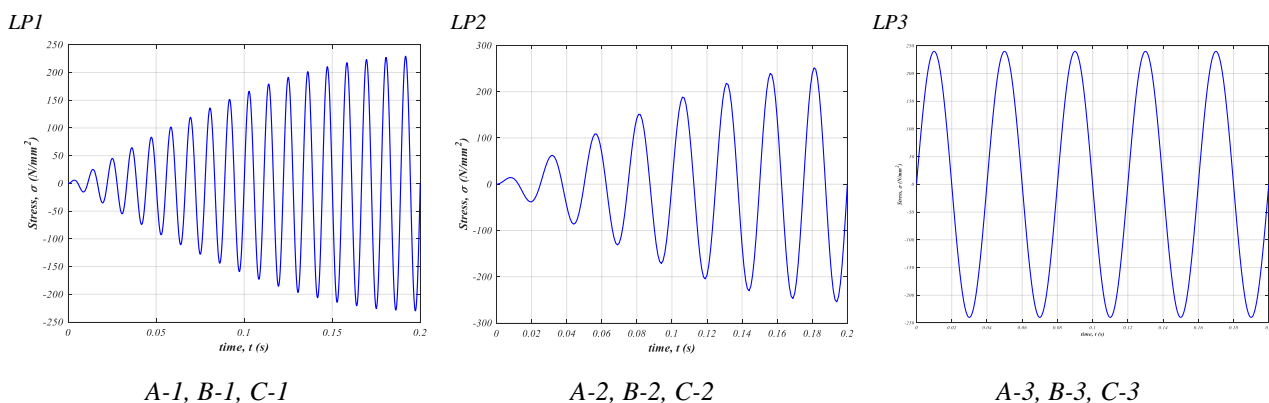


Fig. 1. Cyclic loading patterns (LP)

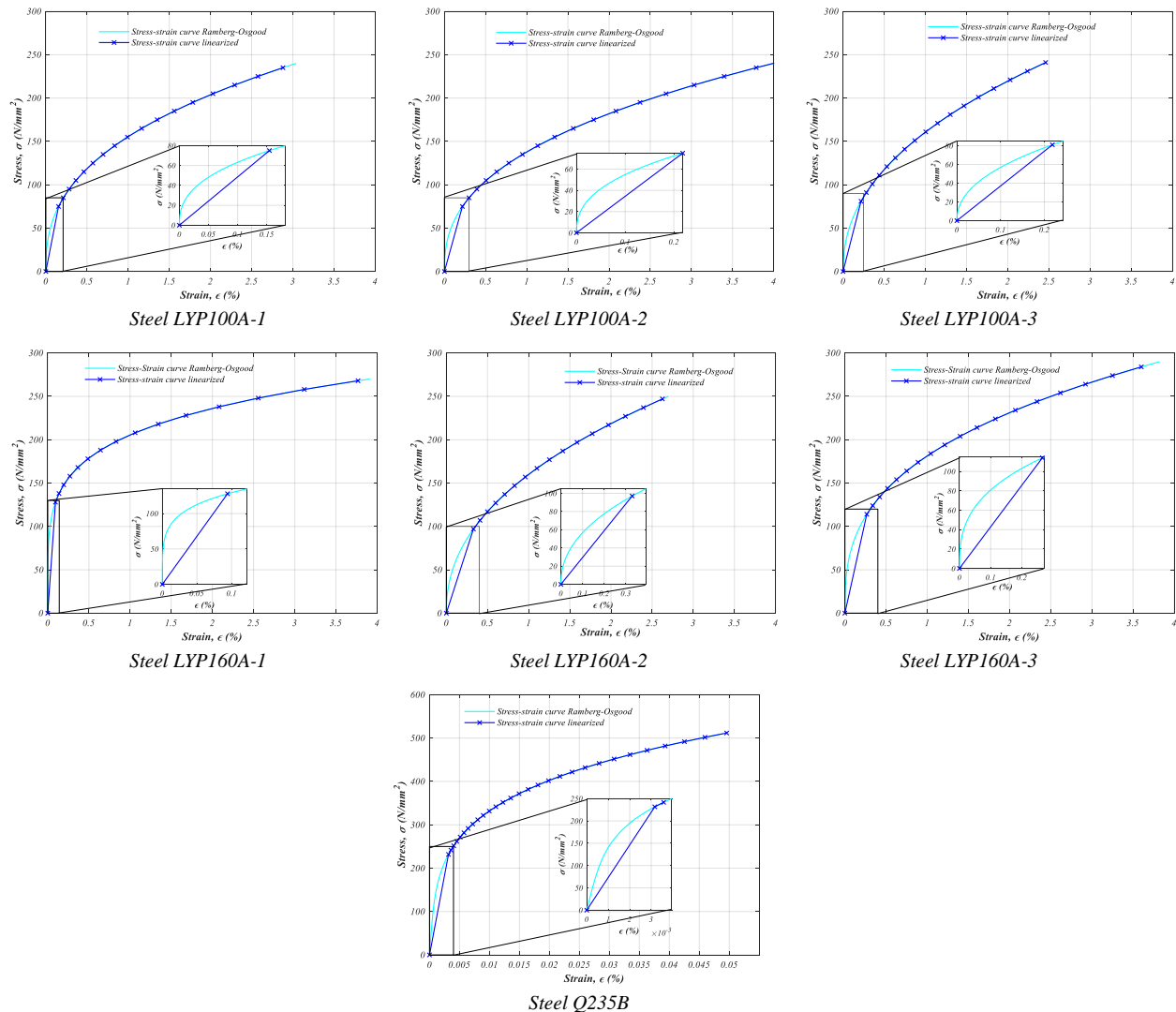


Fig. 2. Stress-Strain curve by Ramberg-Osgood, steels LYP100, LYP160 and Q235B

II. NUMERICAL SIMULATION

A. Materials

The materials considered in this study were two low-yield steels (LYP100 and LYP160) and a conventional steel (Q235B), with the mechanical properties and chemical compositions shown in Tables I and II. The symbols E , f_y , f_u , ϵ , K' , n' , which denote the elastic modulus, yield point, ultimate strength, ultimate deformation, cyclic force coefficient and the cyclic force exponent, respectively. The mechanical properties and chemical composition of the materials were obtained in [23] and [25].

The steels show moduli of elasticity very similar to each other; however, in the inelastic range the LYP steels are very different from conventional steel. The values in Table I show that LYP steels have a higher tensile strength than conventional steel; these values are almost double, indicating greater elongation and good performance in seismic design applications that require a high ductility.

From Table I it can be seen that the yield stress is on average 31% with respect to the ultimate yield stress for the LYP100 steel and major than 38% for the LYP160 steel, indicating an

improvement in the ductility of the latter steel. Based on the responses of the material under cyclic loads obtained in [23] and [25], they were used to apply them to the non-linear cinematic model of Mróz-Garud.

B. Cyclic behavior

The behaviour of the LYP and Q235B steels were studied under a variety of cyclic loading patterns, in order to describe the possible loading conditions in the engineering application and seismic load characteristics, which are shown in Fig. 1. In general terms, all the curves are complete and stable with a significant hardening, which indicates a good energy dissipation capacity. Within each cycle, the post-fluency modulus is very low, and the behaviour is dominated by isotropic hardening, which corresponds to the yield surface. LP1 and LP2 consist of a monotonically increasing strain amplitude with one cycle at each level, and the samples (A-1, A-2, B-1, B-2, C-1 and C-2) tested under these protocols clearly illustrate the isotropic hardening behaviour with gradual saturation. LP3 is a single-phase constant amplitude pattern, applied to samples A-3, B-3 and C-3. The load pattern is constant in the two phases of the curve, the amplitude of stress has the greatest effect on the isotropic hardening due to the

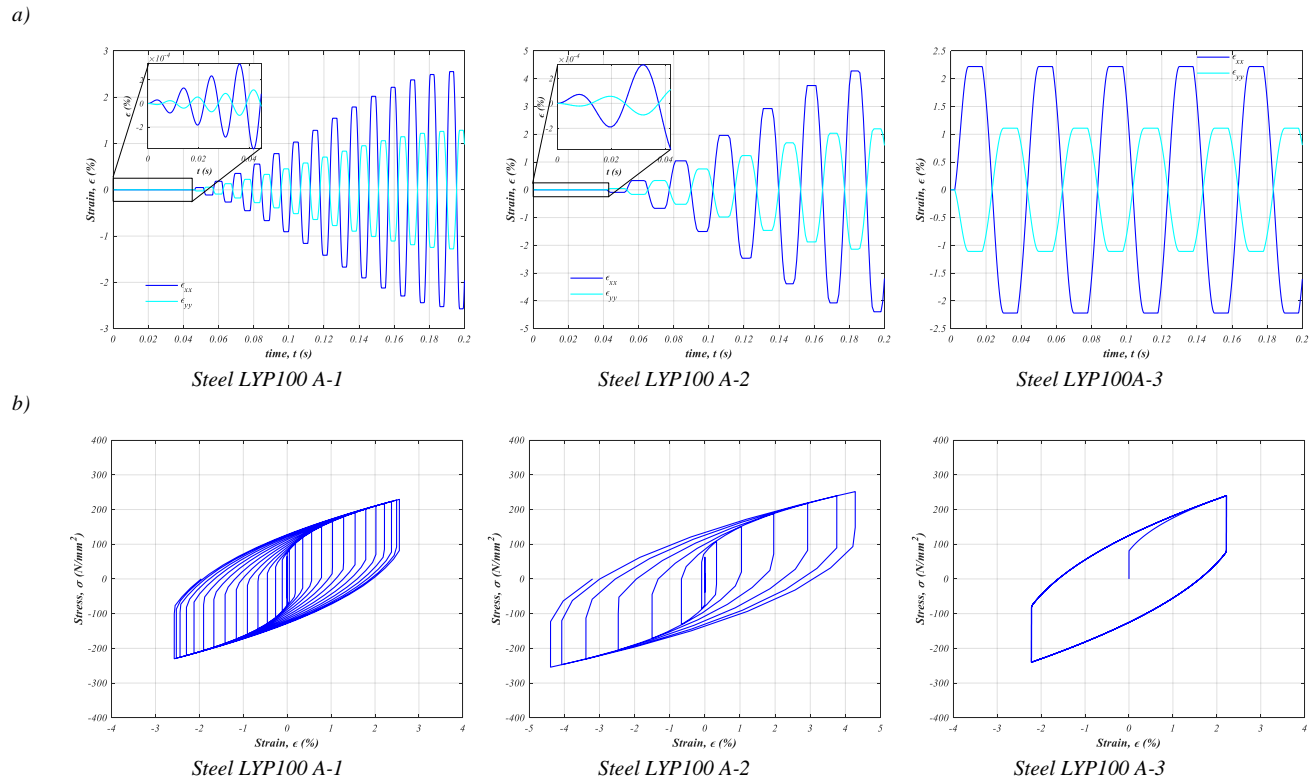


Fig. 3. Simulation results of steel LYP100: a) Strain course, b) hysteresis cycles

amplitude of deformation and the accumulation of plastic deformation, although the accumulation of plastic deformation at a constant amplitude. It also produces hardening. All loading patterns were brought close to the fracture of the material. The stress loads to which they were applied were increasing and decreasing and were calculated every 0.2 milliseconds.

Load and initial tensions. In simulation, as in experimental research [26], the force signal was controlled and given in the form: $F(t) = F_a \sin(2\pi ft)$, where F_a is the amplitude of the force, f is the frequency, and t is the time. The amplitude of the simulated force was equal to 245 N/mm² for LYP steels and 510 N/mm² for Q235B steel, which were high enough to exceed the cyclic creep stress for all materials.

C. Stress-Strain curves

To predict life as a function of stress and strain response for LYP steels, the Ramberg-Osgood model was applied [27], which provides an exponential way to fit an effort-strain curve without an elastic limit and Express of the following equation

$$\varepsilon_a = \varepsilon_{ae} + \varepsilon_{ap} = \frac{\sigma_a}{E} + \left(\frac{\sigma_a}{K'}\right)^{\frac{1}{n'}} \quad (1)$$

where, ε_a and σ_a are the amplitude of the strain and stress, respectively, ε_{ae} and ε_{ap} are the amplitude of the elastic and plastic deformation, respectively, E is the Young's modulus. K' and n' are the cyclic force coefficient and the cyclic force exponent, respectively. The equivalent stress and strain are defined using the von-Mises strain and stress. The stress-strain equation of the total deformation plasticity is given by

where, ε_{ij} is the strain matrix, σ_{kk} is the principal stress matrix, ν is the Poisson's modulus, S_{ij} is the yield stress, ε_{eq}^p is equivalent plastic deformation and σ_{eq} is the equivalent stress. They are calculated as follows

$$\begin{aligned} \sigma_{eq} &= \sqrt{\frac{3}{2} S_{ij} S_{ij}} \\ \varepsilon_{eq}^p &= \sqrt{\frac{3}{2} \varepsilon_{ij}^p \varepsilon_{ij}^p} \\ S_{ij} &= \sigma_{ij} - \frac{1}{3} \sigma_{kk} \delta_{ij} \\ \sigma_{kk} &= \sigma_{11} + \sigma_{22} + \sigma_{33} \end{aligned} \quad (3)$$

For a problem in 2D, the constitutive laws can be simplified as follows:

$$\begin{aligned} \varepsilon &= \frac{1}{E} \sigma + \frac{1}{E_p} \sigma \\ \gamma &= \frac{2(1+\nu)}{E} \tau + \frac{3}{E_p} \tau \end{aligned} \quad (4)$$

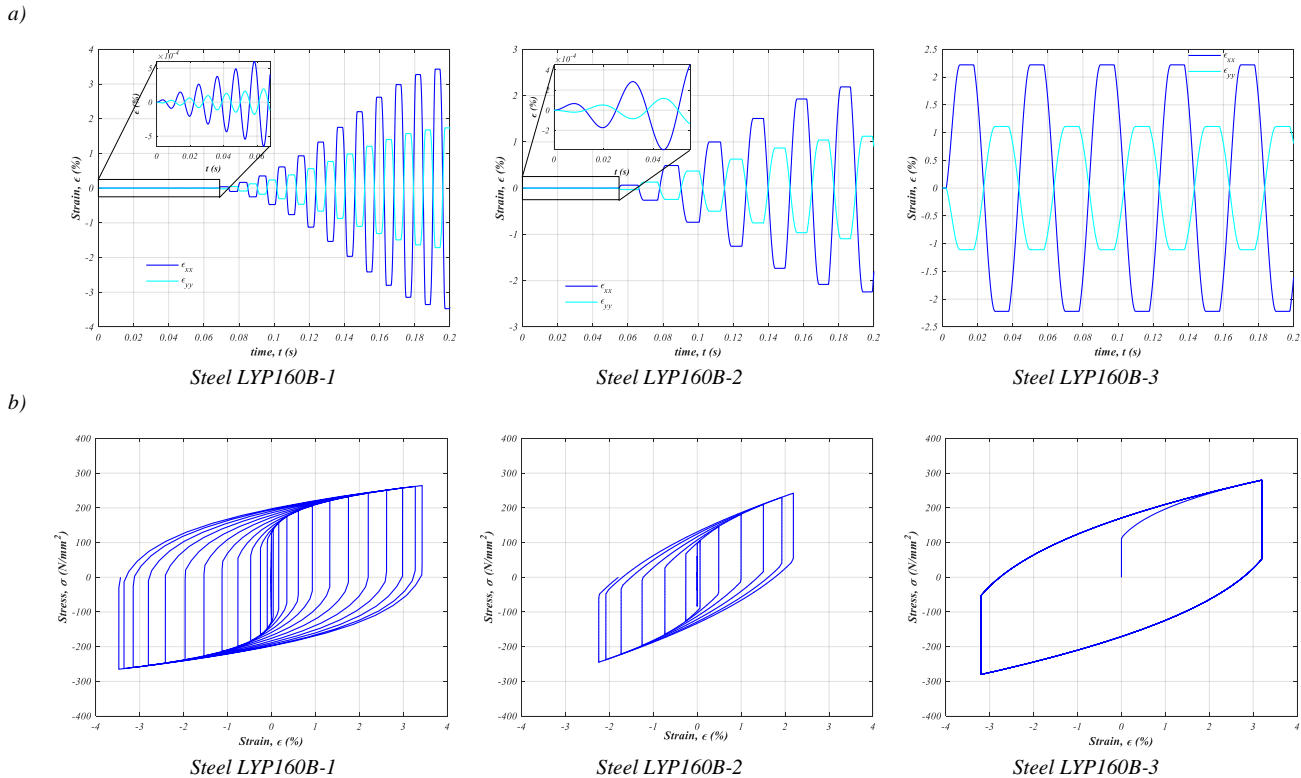


Fig. 4. Simulation results of steel LYP160: a) Strain course, b) hysteresis cycles

where, γ is the shear total deformation, E_p is plastic modulus of elasticity and is defined as $E_p = \frac{\sigma_{eq}}{\epsilon_p} = \frac{\sigma_{eq}}{\left(\frac{\sigma_{eq}}{K}\right)^{\frac{1}{n}}}$, τ is the shear stress.

The equation (4) is the solution for cases of proportional loading, and the stress / strain responses can be obtained for the multiaxial fatigue model. The cyclic parameters of the steels LYP100 and LYP160 were given in Table 1. These were used to perform the simulation using the cyclic loading patterns and the Ramberg-Osgood model, the stress-strain curves were obtained, which are shown in

Fig. 2. he results show consistency with that published by [23] and [24]. According to [23], the maximum cyclic force of the LYP100 steel shows an increase by approximately 80% compared to the monotonic resistance, while the LYP160 steel is observed an increase of 40% compared to the monotonic resistance.

The applied load patterns led to the isotropic softening of the deformation, where the stress-strain cycles were reduced at very small intervals of effort. This phenomenon illustrates the dependence of the shape of the load trajectory on the cyclical stress-strain response of these steels, including the effects related to the sequence, number of cycles, accumulated plastic deformation, stress and the amplitude of effort.

III. CYCLIC MODEL

As it could be observed, LYP steels have a unique cyclic constitutive behaviour, so, it is imperative that, in structural simulations, a good model that represents their behaviour is counted. Based on the results of the previous section, the parameters are determined to simulate the behaviour of the LYP

steels, using the model by non-linear kinematic hardening of Mróz-Garud.

A. Mróz-Garud model

In this work we used the kinematic hardening rule proposed by Mróz [28] and Garud [29]. This model is based on the concept of the fields of modules of constant plasticity. According to this idea, the non-linear stress-strain uniaxial curve ($\sigma_a - \epsilon_a$) roposed by Ramberg-Osgood, equation (2), introduces the plastic module, where, the Ramberg-Osgood curve is treated as a basis of the stress-strain relationship and is approximated by several line segments in the Mróz-Garud model. Each line has its own plastic module H, that is, its line slope is different for different segments. The Mróz model only assumes kinematic hardening and the original rule [28] was modified by Garud [29] to avoid the intersection of the possible performance surfaces in the original concept.

This approach was applied to the stress-strain curves of Ramberg-Osgood, and according to the approximate stress-strain curve, the plasticity surfaces are defined in the stress space corresponding to the stress points in the approach lines. Usually, the inner surface is the yield surface, and the plastic modulus H of the first surface is equal to the Young's modulus of the material. The model introduces several yield surfaces with the size parameter $R^{(i)}$. For an initially isotropic material, the production surfaces are concentric, and the material is homogeneous, isotropic and the influence of the loading speed can be neglected. The model does not include thermal phenomena and assumes that the Young's modulus and the Poisson's ratio are constant.

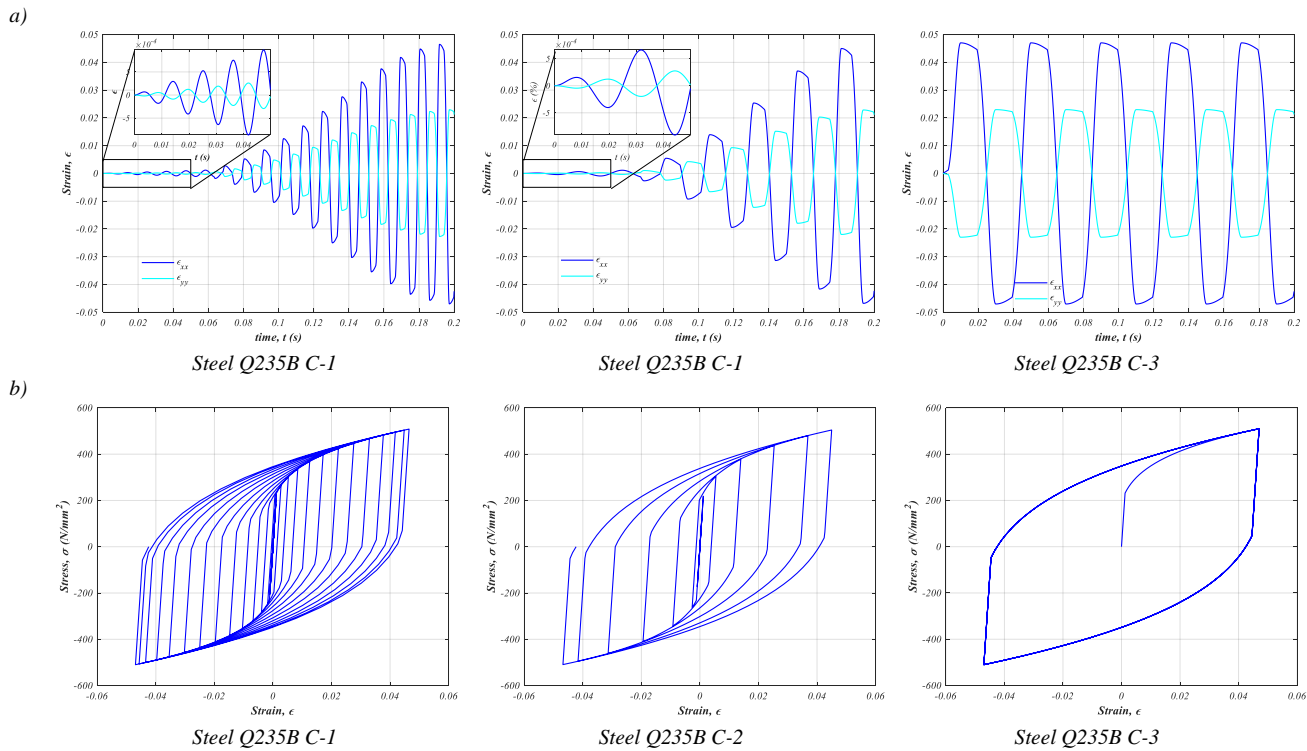


Fig. 5. Simulation results of steel Q235B: a) Strain course, b) hysteresis cycles

When introducing several yield surfaces, the model uses the Huber-Mises Hencky fluency criterion (HMN) applying it in the following way

$$f^{(i)}(s, a^{(i)}, R^{(i)}) = (3/2)(s - a^{(i)}) : (s - a^{(i)}) - R^{(i)^2}, (i = 1, \dots, m) \quad (5)$$

where, s is the stress deviator, $a^{(i)}$ is the recoil stress of the i -th fluency surface (the symbol ':' signifies the scalar product of stress tensors).

Having the initial positions of the yield surfaces and the components of the initial stresses, the cyclically controlled load was implemented in the form of incremental steps the first hysteresis cycles, using the flow rule as follows

$$d\varepsilon^p = \frac{1}{H^{(i)}}(ds : n) \cdot n \quad (6)$$

where, $d\varepsilon^p$ is the increase of plastic deformation, ds is the increase of deviation of efforts, $n = \frac{\partial f}{\partial s} / \sqrt{\frac{\partial f}{\partial s} : \frac{\partial f}{\partial s}}$

Based on equations (5) and (6) the stress and strain components of the LYP steels are obtained, in addition to the hysteretic behaviour of the steels, which are shown in Fig. 3 y 4. In these figures both steels have a cyclic hardening, the LYP100 steel exhibits a higher degree of hardening than the LYP160 steel. When analysing the hardening of these steels, the stress ratio between the yield strength and ultimate stress is 3.19 and 2.63 for the steels LYP100 and LYP160 respectively, while for steel Q235B the ratio is 2.22, indicating a greater ductility in the LYP steels than in conventional steel.

This important phenomenon of isotropic hardening of steels must be taken into account in seismic design, especially when using procedures based on the protection of non-structural elements. The high ductility presented by LYP steels favours the dissipation of energy, due to the greater number of cycles they present compared to conventional steels, this can be seen when comparing the hysteretic behaviour of LYP steel (Fig. 3b and 4b) with respect to the figures of the conventional steel Q235B (Fig. 5b).

B. Cyclic behavior

The curves obtained by the Ramberg-Osgood model are shown superimposed on the hysteresis curves, Fig. 6. The curves of the model go through most of the points of the stress-strain hysteresis cycles, which adapt well enough to the cyclical stress-strain curves obtained by the Mróz-Garud model.

As other authors have described, the behavior of LYP steels subject to cyclic loading may differ due to the behavior of monotonic charges. In this simulation, it is observed that the stress-strain curves obtained with the Ramberg-Osgood method and the Mróz-Garud model show small differences, adequately describing the behavior of the LYP and Q235B steels. There is a small difference, which is due to an isotropic softening of the deformation, where the stress and strain cycles were reduced with progressively small deformation intervals, indicating the dependence of the trajectories of the stress-strain cyclic response for the LYP steels, including the number of cycles, sequence, accumulated plastic deformation, effort and the amplitude of it.

The results indicate that the hardening behaviour of LYP steels is caused by a combination of isotropic and kinematic hardening, although the latter to a lesser extent. It should be noted in Fig. 6 that LYP steels show a greater number of cycles

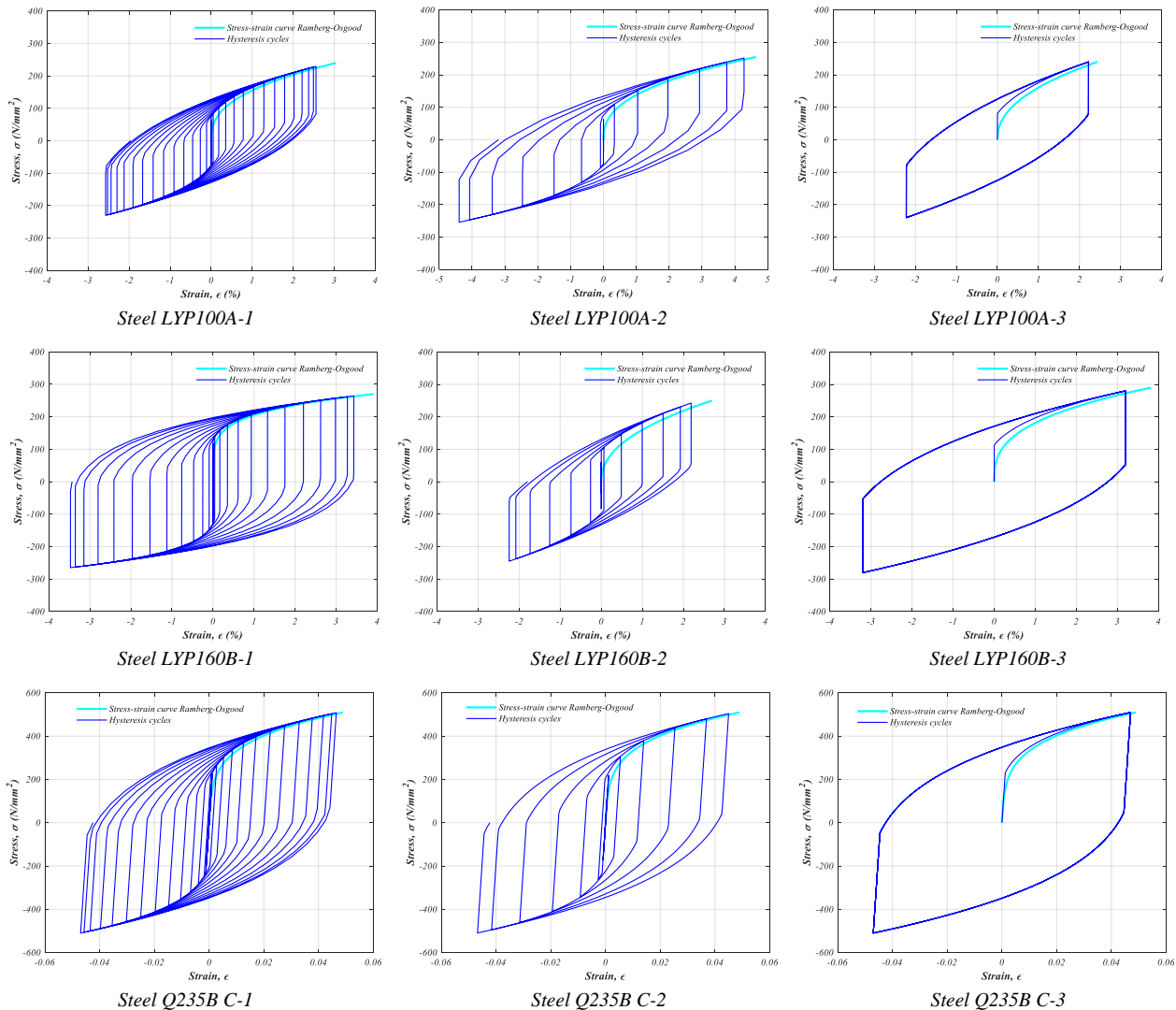


Fig. 6. Hysteresis and cyclic stress-strain curves of steel LYP y Q235B

than conventional steels under the same deformation amplitudes, indicating greater strength and as a result, a higher energy dissipation capacity.

IV. CONCLUSIONS

In this research work, simulations of steels with low yield point were made, specifically the steels LYP100, LYP160 and a conventional steel Q235B under several load patterns using the non-linear kinematic model of Mróz-Garud, focusing on the behaviour cyclic, hardening by deformation and the ability to dissipate energy. The application of the nonlinear kinematic model for fields of stress takes into account the influence of the load history, as a result, the amplitudes of effort are more attached to the practice than the amplitudes of effort. With the implementation of the Mróz-Garud model, significant evidence was obtained to compare with experimental results recently published by other authors. Based on these results, the following conclusions can be drawn:

1. Because the model takes into account the load history, the results show an approximation improvement when there is a greater number of frequencies;
2. The stress-strain curve calculated with the Ramberg-Osgood model can be characterized for LYP steels, allowing its use as a reference for analysis and design;
3. LYP steels show a hardening behaviour by deformation much higher than the typical range in steels Q235B, increasing up to two or three times their resistance to tension;
4. The simulation of LYP steels under cyclic loading, show a good approximation to what has been published by other authors. The phenomena of hardening by cyclic deformation are significant when evaluating them, since, they show a small difference in the cyclical stress-strain curves, adding a small dissipation of additional energy, due to the hardening by cyclic deformation; and
5. Based on the results obtained and reported by other authors in the current literature, the non-linear kinematic model of Mróz-Garud could be used as a tool to approximate the behaviour of LYP steels.

ACKNOWLEDGMENT

The authors wish to express their gratitude to the Autonomous University of the State of Hidalgo for their financial support.

REFERENCES

- [1] D. R. Teruna, T. A. Majid, and B. Budiono, "Experimental study of hysteretic steel damper for energy dissipation capacity," *Adv. Civ. Eng.*, vol. 2015, no. Figure 2, 2015.
- [2] B. Briones and J. C. de la Llera, "Analysis, design and testing of an hourglass-shaped copper energy dissipation device," *Eng. Struct.*, vol. 79, pp. 309–321, Nov. 2014.
- [3] A. S. Whittaker, V. V. Bertero, C. L. Thompson, and L. J. Alonso, "Seismic testing of steel plate energy dissipation devices," *Earthq. Spectra*, vol. 7, no. 4, pp. 563–604, 1991.
- [4] A. Whittaker, V. Bertero, J. Alonso, and C. Thompson, "Earthquake simulator testing of steel plate added damping and stiffness elements," no. December 1988, p. 208, 1989.
- [5] S.-H. Oh, Y.-J. Kim, and H.-S. Ryu, "Seismic performance of steel structures with slit dampers," *Eng. Struct.*, vol. 31, no. 9, pp. 1997–2008, Sep. 2009.
- [6] M. Wang, W. Yang, Y. Shi, and J. Xu, "Seismic behaviors of steel plate shear wall structures with construction details and materials," *J. Constr. Steel Res.*, vol. 107, pp. 194–210, Apr. 2015.
- [7] G.-Q. Li, M. Pang, F. Sun, and J. Jiang, "Study on two-level-yielding steel coupling beams for seismic-resistance of shear wall systems," *J. Constr. Steel Res.*, vol. 144, pp. 327–343, May 2018.
- [8] J. Zhang and T. Zirkalian, "Probabilistic assessment of structures with SPSW systems and LYP steel infill plates using fragility function method," *Eng. Struct.*, vol. 85, pp. 195–205, Feb. 2015.
- [9] T. Zirkalian and J. Zhang, "Buckling and yielding behavior of unstiffened slender, moderate, and stocky low yield point steel plates," *Thin-Walled Struct.*, vol. 88, pp. 105–118, Mar. 2015.
- [10] T. Zirkalian and J. Zhang, "Seismic design and behavior of low yield point steel plate shear walls," *Int. J. Steel Struct.*, vol. 15, no. 1, pp. 135–151, 2015.
- [11] T. Zirkalian and J. Zhang, "Structural performance of unstiffened low yield point steel plate shear walls," *J. Constr. Steel Res.*, vol. 112, pp. 40–53, Sep. 2015.
- [12] F. Perri, C. Faella, and E. Martinelli, "Cost-competitive hysteretic devices for seismic energy dissipation in steel bracings: Experimental tests and low-cycle fatigue characterisation," *Constr. Build. Mater.*, vol. 113, pp. 57–67, 2016.
- [13] M. Dehghani, R. Tremblay, and M. Leclerc, "Fatigue failure of 350WT steel under large-strain seismic loading at room and subfreezing temperatures," *Constr. Build. Mater.*, vol. 145, pp. 602–618, 2017.
- [14] J. L. Li, Y. N. Tang, and X. M. Liu, "Research on dissipation and fatigue capacity of nonstiffener shear panel dampers," *Adv. Civ. Eng.*, vol. 2015, 2015.
- [15] C. Zhang, J. Zhu, M. Wu, J. Yu, and J. Zhao, "The lightweight design of a seismic low-yield-strength steel shear panel damper," *Materials (Basel)*, vol. 9, no. 6, 2016.
- [16] S. Fan, Z. Ding, L. Du, C. Shang, and M. Liu, "Nonlinear finite element modeling of two-stage energy dissipation device with low-yield-point steel," *Int. J. Steel Struct.*, vol. 16, no. 4, pp. 1107–1122, 2016.
- [17] A. Al Kajbaf, N. Fanaie, and K. Faraji Najarkolaie, "Numerical simulation of failure in steel posttensioned connections under cyclic loading," *Eng. Fail. Anal.*, vol. 91, pp. 35–57, Sep. 2018.
- [18] J. L. Chaboche, "Time-independent constitutive theories for cyclic plasticity," *Int. J. Plast.*, vol. 2, no. 2, pp. 149–188, 1986.
- [19] F. Hu, G. Shi, and Y. Shi, "Constitutive model for full - range elasto - plastic behavior of structural steels with yield plateau : Formulation and implementation," *Eng. Struct.*, 2016.
- [20] F. Hu, G. Shi, and Y. Shi, "Constitutive model for full-range elasto-plastic behavior of structural steels with yield plateau: Calibration and validation," *Eng. Struct.*, vol. 118, pp. 210–227, 2016.
- [21] G. Shi, Y. Gao, X. Wang, and Y. Zhang, "Mechanical properties and constitutive models of low yield point steels," *Constr. Build. Mater.*, vol. 175, pp. 570–587, Jun. 2018.
- [22] L. Yang, Y. Gao, G. Shi, X. Wang, and Y. Bai, "Low cycle fatigue property and fracture behavior of low yield point steels," *Constr. Build. Mater.*, vol. 165, pp. 688–696, 2018.
- [23] M. Wang, L. A. Fahnestock, F. Qian, and W. Yang, "Experimental cyclic behavior and constitutive modeling of low yield point steels," *Constr. Build. Mater.*, vol. 131, pp. 696–712, 2017.
- [24] Y. Chen, W. Sun, and T. M. Chan, "Cyclic stress-strain behavior of structural steel with yield-strength up to 460 N/mm²," *Front. Struct. Civ. Eng.*, vol. 8, no. 2, pp. 178–186, 2014.
- [25] Integrated Systems Research, "Estimating notch strain with net section plasticity," 1999. [Online]. Available: <https://www.isrtechnical.com/?page=TechBrief>. [Accessed: 05-Jun-2018].
- [26] A. Karolczuk, M. Kowalski, R. Banski, and F. Zok, "Fatigue phenomena in explosively welded steel – titanium clad components subjected to push – pull loading," vol. 48, pp. 101–108, 2013.
- [27] W. Ramberg and O. W. R., "Description of Stress-Strain Curves by Three Parameters." National Advisory committee for Aeronautics, Washinton, p. 29, 1943.
- [28] Z. Mróz, "On the description of anisotropic workhardening," *J. Mech. Phys. Solids*, vol. 15, no. 3, pp. 163–175, 1967.
- [29] Y. S. Garud, "A New Approach to the Evaluation of Fatigue Under Multiaxial Loadings," *J. Eng. Mater. Technol.*, vol. 103, no. 2, p. 118, 1981.